Journal of Polymers and the Environment (2019) 27:1828–1842
https://doi.org/10.1007/s10924-019-01481-4

ORIGINAL PAPER

Effective Adsorption of Cr(VI) by High Strength Chitosan/Montmorillonite Composite Hydrogels Involving Spirulina Biomass/Microalgae

Emre Tekay[1] · Demet Aydınoğlu[2] · Sinan Şen[1]

Published online: 25 May 2019

Abstract
The "3-in-1 type" biopolymer composite (chitosan/montmorillonite clay/biosorbent) hydrogels were produced and used as adsorbents for Cr(VI) ion. Na-Montmorillonite (NaMMT) clay was modified with Spirulina (Sp) biosorbent by using lyophilization based "cryoscopic expansion" (C-XP) method. The Sp immobilized MMT (SpMMT) clay containing hydrogels were found to have an open/extended form of Sp structure on their pores' walls, presenting all possible receptor groups for adsorption of Cr(VI) ions. SpMMT loaded hydrogels showed higher adsorption capacities than NaMMT loaded ones. The physically crosslinked hydrogel including only 1% SpMMT (1SpM-H) clay exhibited 150% higher adsorption capacity as compared to neat chitosan hydrogel even in 50 ppm Cr(VI) solution. The same composite hydrogel was found to adsorp about 780% Cr(VI) with respect to the clay's weight while individual uses of Sp and MMT can remove only about 4.80 and 0.36% Cr(VI) with respect to their weights. The pseudo-first order model was found to be the most suitable for the kinetic data of NaMMT loaded hydrogels while that of SpMMT containing hydrogels followed the pseudo-second order kinetics. The isotherm data of all the hydrogels exhibited a better fit to the Freundlich and Sips model. The maximum adsorption capacity (3333 mg g^{-1}) calculated by Sips model was achieved via the hydrogel having 1% SpMMT which is in good agreement with the experimental kinetic data. The highest adsorption with the lowest amount of SpMMT clay could be attributed to its looser Sp network structure whose functional groups are in long-distance, releasing more adsorption sites for the Cr(VI). The highest compression modulus and toughness were also obtained with the 1SpM-H hydrogel which is probably due to increased physical and reversible interactions between chitosan molecules and SpMMT clay layers at optimum clay loading (1%).

Keywords Biopolymer · Composite hydrogel · Adsorption · Chromium(VI) · Mechanical properties

Introduction

Hexavalent Cr(VI) is present in industrial wastes as chromate CrO_4^{-2}, dichromate $Cr_2O_7^{-2}$, $HCrO_4^-$ and H_2CrO_4 [1] depending on the pH of the medium, and toxic even at low concentrations. Cr(VI) is a carcinogenic substance due to its mutogenic property [2]. The adsorption method was performed for Cr(VI) ion with different adsorbents such as fungus [3], green algae [4], bentonite [5] and composite hydrogel [6]. In recent years, applications of biotechnologies in the removal and control of metal pollution have attracted much attention due to their easy applicability and low cost. Biosorption is an alternative biotechnological process in which various biobased/natural materials are used [7]. In the biosorption method, various species such as bacteria, algae, fungi, yeast as biomass (biosorbent) have been used alive or dead [7]. Spirulina biosorbent/biomass with a porous three-dimensional network structure includes protein/lipid and polysaccharide hydrophobic molecules with amine, carboxylic, hydroxyl, phosphate, and sulfate functional moieties, which make it highly attractive in adsorption process [8–10]. Its polar functional groups also have capability of formation of hydrogen bonding with chitosan molecules as additional crosslinks, resulting a co-network structure on the walls of chitosan matrix cells [9]. The adsorption capacity of the Sp to the metal surface alone has been demonstrated

✉ Sinan Şen
sinans@yalova.edu.tr

[1] Department of Polymer Engineering, Yalova University, 77100 Yalova, Turkey

[2] Department of Food Process Technologies, Yalova University, 77500 Yalova, Turkey

in many studies in the literature. Chojnacka et al. [10] examined the adsorption of Cr^{3+}, Cd^{2+}, and Cu^{2+} ions using Sp biomass. The results showed that the structural morphology of Sp, which is dependent on the pH-dependent functional groups of the cell walls, affects the metal adsorption capacity. The lyophilized form of Spirulina was found to adsorb the highest amount of Cr^{3+} and Cu^{2+} ions. In a study by Doshi et al. [11], the maximum Cr(VI) adsorption capacity of Sp biosorbent was reported to be 48 mg Cr(VI) per g Spirulina for 2000 ppm solution concentration.

The chitosan biopolymer has been widely used in preparation of hydrogels because of its hydrophilic character with its amine and hydroxyl groups, and its physical cross-linking ability [12–14]. However, chitosan-based hydrogels have low mechanical strength, especially in their swollen form, due to the weak network of linear polysaccharide molecules [15]. These weaknesses limit their use in applications where high stress is required [16]. To eliminate this disadvantage, studies involving the incorporation of nano-sized enhancers such as hydroxyapatite [17, 18], nano-sized clay [19], carbon nanotube [20], titanium [21] and graphene [22] into natural polymers such as chitosan have been carried out. In our previously published paper [8], a chitosan composite hydrogel based adsorbent system having Sp microalgae immobilized on halloysite nanotube was reported. The modification of the nanotubes with Sp via conventional solution mixing method provided higher swelling, toughness and compression modulus as well as higher Cr(VI) adsorption capacity as compared to neat chitosan and unmodified nanotube containing hydrogel. The enhanced adsorption was attributed to formation of an optimized special morphology of Sp-chitosan composite hydrogel in which all the functional moieties of physically crosslinked Sp biomass at cell walls and the nanotubes act as receptor domains for chromate anions. In another study, we reported styrene-based HIPE (high internal phase emulsion)-templated polymer composites [23] in which immobilization of Spirulina algae to the surface of the NaMMT clay was performed with a new cryoscopic expansion method (C-XP) unlike the above-mentioned conventional solution method. In C-XP method, immobilization of Sp to the clay surface was performed by a sublimation technique in a freeze-lyophilizer using relatively a much smaller amount of solvent. In addition, since the C-XP method uses a lyophilizer for drying, there is no need for drying under heat and laborious procedures such as centrifugation or filtration [23]. In a recent study, biopolymer based nanofibers were prepared by using chitosan and tannin biopolymers with nylon 6 polymer and used for removal of chromium (VI) [24]. The adsorption capacity of the tannin/nylon 6 nanofibers for Cr(VI) was found to be higher than the chitosan/nylon 6 nanofibers. The maximum metal adsorption capacities of tannin/nylon 6 nanofibers and chitosan/nylon 6 at 25 °C were obtained as about 40 mg/g and 14 mg/g, respectively. The higher adsorption performance of tannin/nylon 6 system was attributed to presence of many hydroxy phenolic moieties leading to a chelate compound with metal ions.

In this project, Sp immobilized MMT clay, which is obtained via the C-XP method [23], is used in preparation of novel physically crosslinked chitosan composite hydrogels with high mechanical strength. It was expected that C-XP assisted immobilization of Spirulina algae on the MMT surface will contribute to the physical cross-linking of the polymer with its functional groups (polysaccharide molecules, amino acids and other ionic structures) [9]. Also, these interactions were believed to increase heavy metal removal performance of this novel and triple biopolymer/biomass/layered silicate (chitosan/spirulina/MMT) hydrogel adsorban system. Swelling and metal adsorption capacities, morphological properties and mechanical properties of hydrogels were examined as a function of clay type and its percentage.

Experimental

Materials

The chitosan polymer was obtained from Aldrich Chemicals (Milwaukee, US). The degree of deacetylation of chitosan (DD) is in the range of 75–85% and has a viscosity in the range of 200–800 cps. Sodium montmorillonite (NaMMT) clay was obtained from Süd-Chemie (Steinheim, Germany) with a brand name of Nanofil 1080. Acetic acid, sodium hydroxide, potassium dichromate ($K_2Cr_2O_7$) and diphenyl carbazide were purchased from Aldrich Chemicals (Milwaukee, US). Spirulina (Sp) was bought from Egert Natural Products Production Limited Company (İzmir, Turkey).

Modification of Montmorillonite Clay by Spirulina

Modification of NaMMT clay was performed by cryoscopic expansion (C-XP) method as reported in our previously published paper [23]. Individual solutions of 1 g of NaMMT and 0.05 g of Spirulina in 10 ml of deionized water were prepared. The solutions were stirred at 50 °C for 1 h with a magnetic stirrer. At the end of the period, the Sp solution was added onto the MMT clay solution. The resulting mixture was stirred at 50 °C for 1 h and frozen at − 20 °C. The frozen solution was dried for 48 h in a lyophilizer. Thus, organophilic MMT clay (SpMMT) was obtained.

Preparation of Chitosan Composite Hydrogels

SpMMT filled chitosan hydrogels were prepared by using SpMMT clay ranging from 1 to 5% by weight. First, the SpMMT clay was dispersed in 10 mL of 1% (v/v) acetic acid solution at 25 °C for 4 h and then 0.1 g of chitosan was

added to this solution and dissolved. The mixture was stirred at 25 °C for 3 h. The solution was then poured into polystyrene molds with a diameter and height of 30 mm and 10 mm, respectively. The molds were placed in a cooler at − 20 °C and frozen, and lyophilized at − 45 °C and 0.017 mbar. After lyophilization, all the hydrogels were neutralized by putting them in 1 M NaOH solution for one hour. They were then washed with plenty of deionized water to complete the purification process. The hydrogels were again subjected to the abovementioned drying steps in the lyophilizer. Neat chitosan hydrogel and composite hydrogels with NaMMT clays were also prepared by appyling the same procedure. NaMMT filled chitosan hydrogels were named as xM-H while SpMMT filled hydrogels were named as xSpM-H where x represents clay loading degree (wt %). Neat chitosan hydrogel was named as Ch-H.

Characterization

Measurements of the basal distances between the crystalline layers of pure NaMMT clay and organophilic SpMMT clay were done by X-ray diffraction (XRD, Rigaku D/Max-Ultimate diffractometer, CuK_{α} radiation, $\lambda = 1.54°A$, Rigaku, Tokyo, Japan) analysis at a speed of $2° \text{ min}^{-1}$ at 40 mA and 40 kV operating conditions. Thermogravimetric analyses (TGA) of NaMMT and SpMMT clays were performed in the range of 30 °C to 700 °C, at a heating rate of 10 °C min^{-1} and under a nitrogen atmosphere by using a TG analyzer (Seiko TG/DTA 6300, Seiko Instruments Inc., Tokyo, Japan). The XRD curves and TGA thermograms together with their data were given and discussed in our previously published work [23].

Morphological characterization of the clays and hydrogels were done by scanning electron microscope (SEM) (ESEM-FEG and EDAX Philips XL-30, Philips, Netherlands).The swelling ratios of the hydrogels were calculated gravimetrically after 24 h in beakers containing deionized water. Since the hydrogels are physically cross-linked, a time-dependent monitoring was not performed, but swelling test was performed with a single measurement after 24 h. The Swelling percentage (S %) were calculated using the following formula:

$$S\% = \frac{m_s - m_0}{m_0} \times 100 \tag{1}$$

where m_s and m_0 refer to the mass of the swollen gel and that of dry hydrogel, respectively.

The mechanical uniaxial compression tests of wet hydrogels were carried out at room temperature and at a rate of 2 mm min^{-1}. The tests were done by the Zwick/Roell Z1.0 Universal Testing Machine (Zwick GmbH & Co. KG, Germany) with a load cell of 50 N until the sample deformation reached 70%.

In order to investigate capability of the chitosan composite hydrogels in the heavy metal removal applications, their Cr(VI) absorption was examined at 25 °C at pH of 5.5–6.0. For this purpose, all the chitosan hydrogels were placed in 50 ppm Cr(VI) solution and, initial Cr(VI) concentrations and those at certain time intervals were determined by using diphenyl carbazide and 3500-Cr technique [25]. The measurements were carried out at 540 nm by UV spectrophotometer (Optizen Pop Spectrophotometer, Daejon, South Korea). In the determination of the adsorption isotherms, the abovementioned measurements were repeated for dry hydrogels which were placed in separate solutions with different Cr(VI) concentrations (50, 100, 150, and 200 ppm). The Cr(VI) absorbed by 1 g of hydrogel was calculated as q_e (mg Cr(VI) per g dry hydrogel) by using the following equation [25]:

$$q_e = \frac{\sum \left(C_i - C_f\right) \times V}{W} \tag{2}$$

In the equation, the C_i and C_f show initial and final concentrations of the metal ions at each time interval in the solution (mg L^{-1}), respectively. V and W represent the volume of the metal ion solution and the dry weight of the hydrogel used in the experiment, respectively.

The pseudo-first-order (Eq. 3) and pseudo-second-order (Eq. 4) kinetic models were used to investigate the kinetics of the adsorption by using the following formulae [13]:

$$q_t = q_e\left(1 - e^{-k_1 t}\right) \tag{3}$$

$$q_t = \frac{t}{(1/k_2 q_e^2) + (t/q_e)} \tag{4}$$

where k_1 (min^{-1}) and k_2 (g mg $^{-1}$ min^{-1}) are the rate constants of pseudo-first-order ans pseudo-second-order rate constants, respectively; q_t and q_e are the amounts of adsorbed Cr(VI) on the hydrogels at time t and at equilibirum.

Equilibrium adsorption results were fitted to Langmuir (Eq. 5) [24], Freundlich (Eq. 6) [24] and Sips (Eq. 7) [14] models:

$$q_e = \frac{q_m K_L C_e}{1 + \left(K_L C_e\right)} \tag{5}$$

$$q_e = K_F C_e^{1/n} \tag{6}$$

$$q_e = \frac{q_m \left(K_s C_e\right)^{n_S}}{1 + \left(K_s C_e\right)^{n_S}} \tag{7}$$

where C_e is equilibrium concentration of Cr(VI) (mg L^{-1}); q_m (mg g^{-1}) and and q_e (mg g^{-1}) are the adsorption capacities at any time and equilibrium, respectively; K_L is the

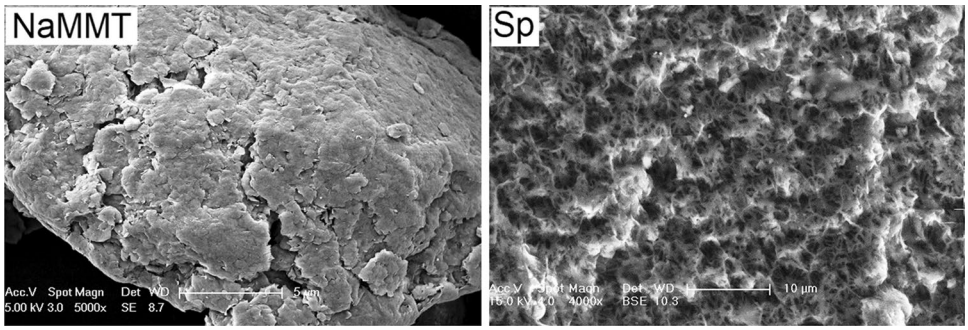

Fig. 1 SEM images of MMT and Spirulina biomass (Sp)

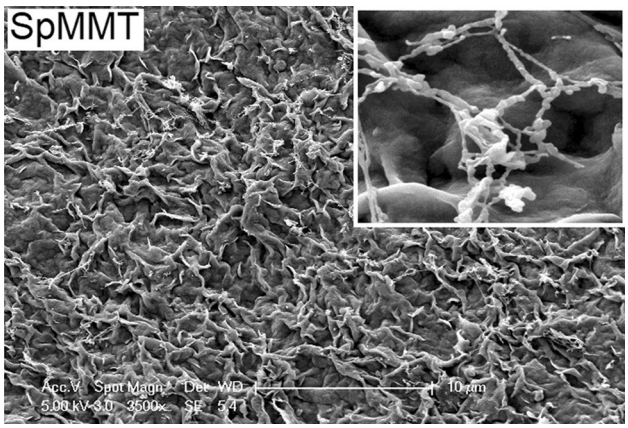

Fig. 2 SEM image of Spirulina immobilized MMT (SpMMT)

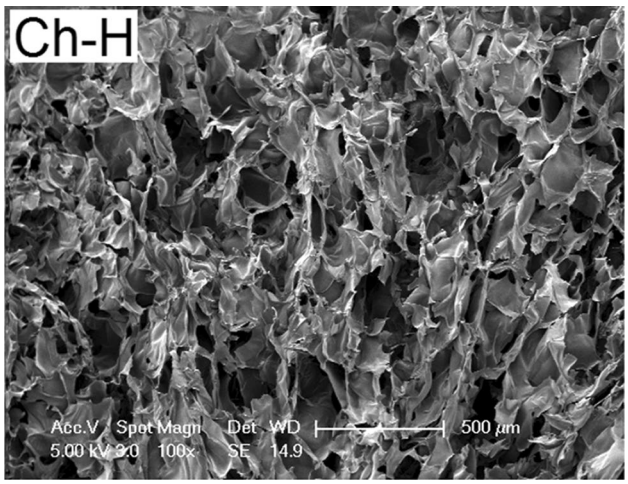

Fig. 3 SEM image of neat chitosan (Ch-H) hydrogel (Mag: × 100)

Langmuir constant; K_F and n are the Freundlich constants related to the adsorption capacity and adsorption inensity, respectively; K_S is (L g^{-1}) is related with the energy of adsorption and n_S is indication of system heterogeneity in the Sips isotherm model.

Results and Discussion

Morphological Characterization of SpMMT Clay and the Hydrogels

SEM image showing micrometer-sized pure NaMMT clay with a smooth surface is given in Fig. 1. It also shows SEM image of Sp biomass, which was used in the clay modification, having a porous and three-dimensional network structure. After the clay modification, the three-dimensional network structure of Spirulina was found to coat the surface of NaMMT clay and transform it to a homogeneous and rough surface (Fig. 2). The network structure of Sp was found to be in an open and extended form in a larger area on the NaMMT surface (Fig. 2-inset figure) [23]. This special morphology obtained by cryoscopic expansion method was expected to cause the functional groups of Spirulina such as amine, carboxyl, hydroxyl, phosphate and sulphate to play a more effective role in heavy metal adsorption process.

Figures 3, 4, 5 shows SEM images of internal surface morphologies of neat chitosan, NaMMT filled hydrogels and SpMMT filled hydrogels, respectively at the same magnifications (Mag: × 100). As it is observed from the Fig. 3 that neat chitosan hydrogel (Ch-H) has a open cell morphology resulting from repulsive forces between protonated amine groups of the molecules together with closed cells due to their possible intramolecular interactions. The 1 M-H hydrogel obtained with 1% NaMMT was found to have open pores together with the still presence of closed pores which is similar to neat hydrogel. It shows a more homegeneous dispersion of pores with a smaller size (Fig. 4), compared to Ch-H hydrogel. This may be ascribed to formation of additional hydrogen bonding and ionic interactions between the negatively charged surface of the NaMMT clay layers and protonated amine groups of the chitosan molecules as physical crosslinks [26]. This leads to a increased crosslinked density and porous structure in the hydrogel system [27]. On the other hand, at higher amount of the NaMMT clay (3 and 5%), the porous structures of the hydrogels were found to be disrupted (Fig. 4) and have almost completely closed

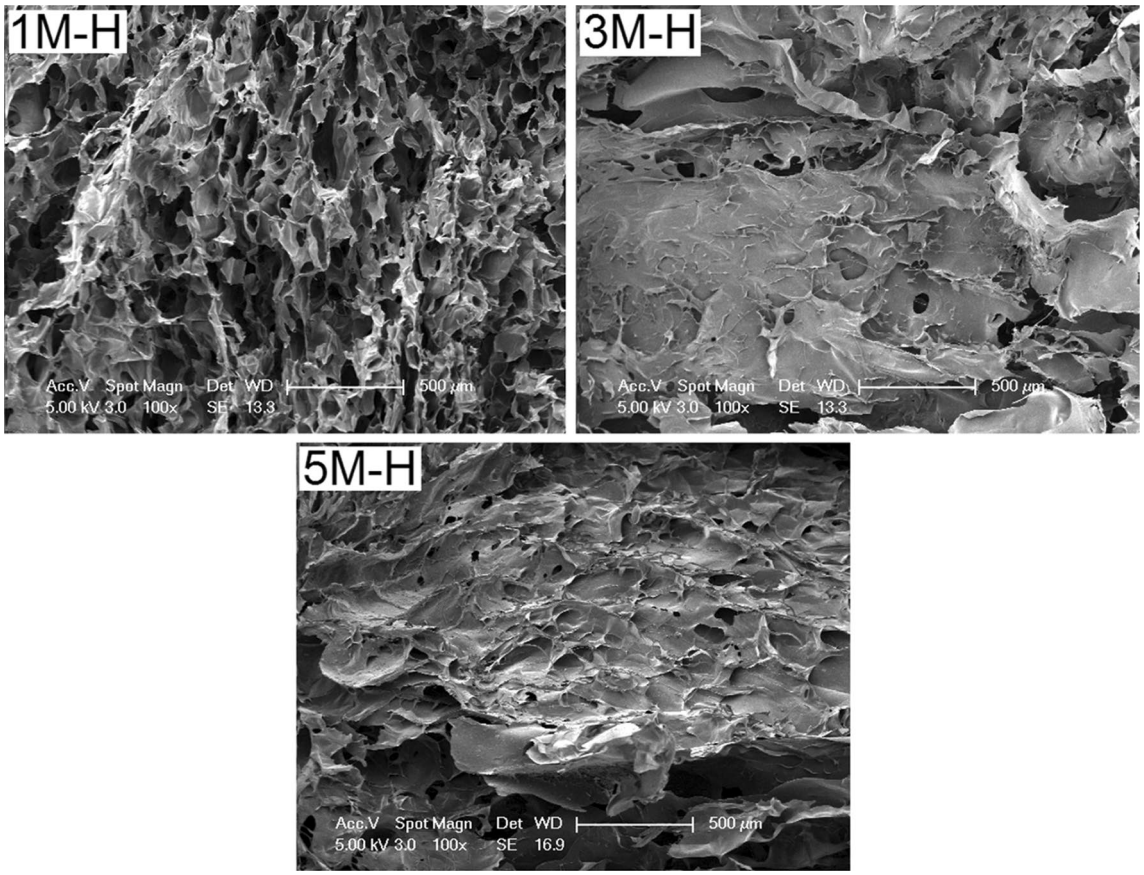

Fig. 4 SEM images of NaMMT loaded composite hydrogels (Mag: × 100)

pores and heterogeneous structures. This can be attributed to relatively more interactions of the hydroxyl, amine and carboxyl groups of the chitosan molecules with silanol groups on the surface of NaMMT clay. It can be also due to the increased abovementioned ionic interactions between chitosan molecules and negatively charged surface of the clay layers at the higher unmodified clay loading. This may decrease the probability of repulsive forces between the protonated amine groups of the chitosan molecules and increase intramolecular inteactions of the chitosan molecules instead of intermolecular ones, destroying the sponge morphology.

The SEM images of SpMMT loaded chitosan composite hydrogels are given in Fig. 5. As it can be seen from the figure, 1SpM-H hydrogel, unlike the 1 M-H hydrogel, exhibited a closed-pore structure with some amounts of open pores. It may be ascribed to interaction of the polymeric chains (polysaccharide and amino acids) of the Sp biosorbent with chitosan molecules, reducing the physical bonds between chitosan chains. On the other hand, when the degree of SpMMT loading was above 1%, a more porous structure with relatively larger and open pores were obtained (Fig. 5). The observed open porous morphologies for the 3SpM-H and 5SpM-H hydrogels can be explained by higher amount of Sp leading to the additional crosslinks giving a porous structure via help of its abovementioned functional groups. These additional non-covalent/physical crosslinks may result from interaction of Sp molecules between themselves and that of Sp and chitosan molecules through dipole–dipole forces and hydrogen bonding. Moreover, the 3SpM-H and 5SpM-H hydrogels were found to have larger pores, as compared to 1SpM-H and the chitosan/NaMMT hydrogels with the same loading degrees. This may be probably due to formation of larger ice crystals formed in the freezing process during preparation of those hydrogels resulting from decrease in their hydrophilicity with hydrophobic structure of Sp biosorbent at higher SpMMT loading [28].

Moreover, at higher magnification (Mag: × 1000) SEM images of the pore walls of the SpMMT loaded hydrogels (Fig. 6), Sp bisorbent molecules were seen to be in an open/extended form and aggregate form in 1SpM-H and 5SpM-H hydrogels, respectively, which were marked with a red circle and showed in the inset figures. On the other hand, both open/extended and aggregate forms of Sp are present in 3SpM-H hydrogel. The effective and beneficial morphology of Sp biosorbent is more clearly seen at much higher magnification SEM images (Mag: × 50,000) of the SpM-H

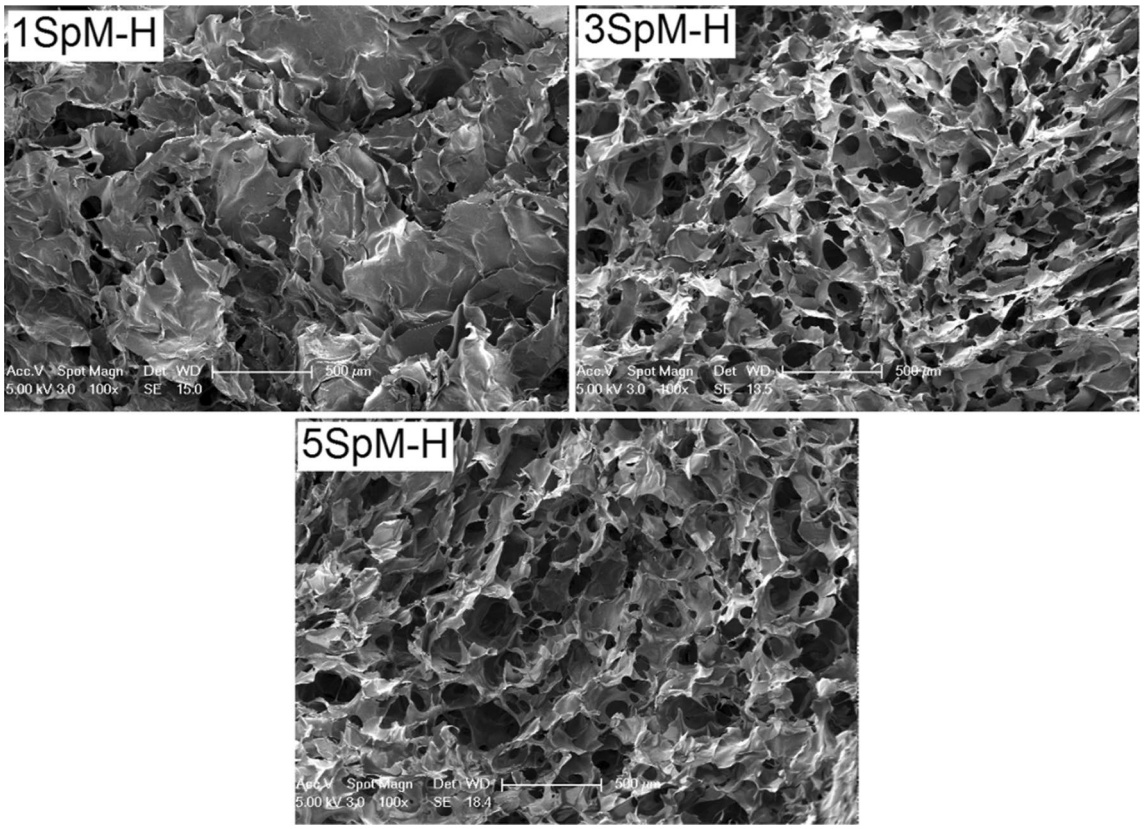

Fig. 5 SEM images of SpMMT loaded composite hydrogels (Mag: × 100)

hydrogels (Fig. 7). It is observed in Fig. 7 that there are some special sub-networks of Sp on the pore walls of the hydrogels. Among SpMMT containing hydrogels, the 1SpM-H shows immobilized spirulina in open form much more presenting all possible potential attachment points for water molecules and metal ions [10].

Swelling Behaviour of Neat Chitosan and Composite Hydrogels

Figure 8 shows the swelling behavior of neat chitosan and chitosan composite hydrogels as a function of NaMMT and SpMMT loading percentages. As can be seen from the graph, all the hydrogels with NaMMT loading have higher swelling ratios than pure chitosan. This can be due to presence of hydrophilic nano-sized silicate layers added to the structure facilitating diffusion of water molecules. On the other hand, when the amount of NaMMT clay is increased to 3%, it is observed that the swelling value decreases. This result may be ascribed to insufficient dispersion of the silicate layers and the closed pores in the structure of the hydrogel at higher loading of the clay (Fig. 4). The reason for the decrease in swelling at 3% loading of NaMMT, as compared to 1% NaMMT loaded hydrogel can be explained by formation of relatively higher amount of hydrogen bonding between chitosan molecules and the clay. The amine, acetamide, or hydroxyl groups of chitosan molecules may form dipole–dipole and hydrogen bonding with Si–O-S/Si–OH groups of the MMT layers. This may decrease the repulsive forces of the chitosan molecules getting them closer and inhibit the water-attractive functional groups of chitosan molecules to adsorp water molecules. It can also be due to high amount of ionic interactions occuring between protonated amine groups of the chitosan molecules and negatively charged surface of the MMT clay. These interactions can also decrease water diffusion and the swelling [27]. In addition, it is thought that cross-linking density may be increased by the formation of additional cross-links resulting from possible ionic interactions between positively charged chitosan molecules and negatively charged MMT surface due to the higher amount of NaMMT loading and thus some reduction in swelling occurs. On the other hand, as seen in the Fig. 8, the swelling ratio increased again when the amount of NaMMT clay was increased to 5%. This result can be ascribed to presence of higher number of open pores for 5 M-H, compared to 3 M-H hydrogels even though both have disrupted porous structures (Fig. 4). Thus, water adsorption capacity of the composite hydrogel may be increased due to the increase in number of the open pores. Moreover, it can be said that the negatively

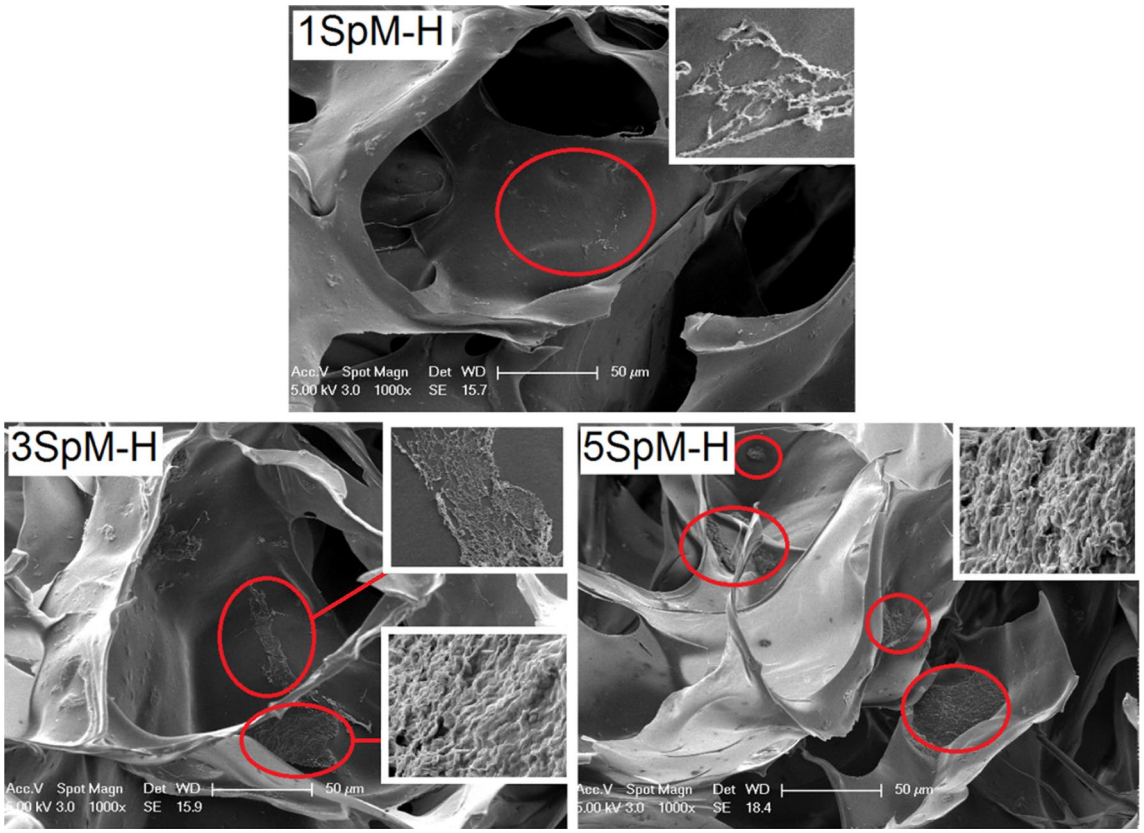

Fig. 6 High magnification (Mag: × 1000) SEM images of pore walls of the SpMMT loaded composite hydrogels

charged groups of MMT clay at 5% loading have caused more possible ion–dipole interactions and swelling with water than the 3% NaMMT loaded hydrogel.

In the SpMMT loaded chitosan hydrogels, swelling ratios were found to be lower than pure chitosan and NaMMT loaded chitosan hydrogels (Fig. 8). This may be related to the abovementioned hydrophobic structure of Spirulina in the SpMMT clay. On the other hand, as for NaMMT loaded hydrogels, a decrease in the swelling ratio with 3% SpMMT clay is observed which can be probably due to the aforementioned reason given for NaMMT loaded hydrogels. Then, the swelling ratio increased again with increased amount of ionic groups at 5% SpMMT loading degree. Furthermore, the organic modification of the MMT clay with the Spirulina molecule results in larger number of functional groups that can interact with water molecules in terms of 5SpM-H hydrogel.

Effect of Time on Metal Adsorption Behaviour of Hydrogels and Kinetic Parameters

Figure 9 shows the heavy metal (Cr(VI)) absorption behavior of neat chitosan and composite hydrogels loaded with NaMMT and SpMMT clays. In aqueous solutions Cr(VI) is available in neutral (H_2CrO_4) and different anionic forms such as $HCrO_4^-$, CrO_4^{-2} and $Cr_2O_7^{-2}$. The ions are generally in the form of $HCrO_4^-$ in the range of pH 2 and 6. When the solution has pH values greater than 6, the anions of CrO_4^{-2} and $Cr_2O_7^{-2}$ become dominant. When the pH is higher than 7.5, the aqueous solution contains only the CrO_4^{-2} anion [29]. By the way, when the pH is lower than 6.2, the chitosan molecule has a positive charge resulting from the protonated amine groups (–NH_2) on it, and this may provide the interaction of NH_3^+ groups with the chromate anions [30].

As shown in Fig. 9, the hydrogels containing 3 and 5% NaMTM clay were found to have lower adsorption values than neat chitosan hydrogel (Ch-H). This can be attributed to their morphologies having closed pores (Fig. 4). It may be also due to relatively higher amount of negatively charged clay layers interacting with the protonated amine groups of chitosan molecules, preventing their adsorption capabilities. In addition, increasing negatively charged MMT surfaces with increasing the degree of NaMMT loading can push the chromate anions and can be effective in reducing the adsorption. On the other hand, 1 M-H hydrogel was found to have higher adsorption capacity than neat chitosan hydrogel and the highest adsorption performance among NaMMT loaded composite hydrogels. The relatively higher adsorption

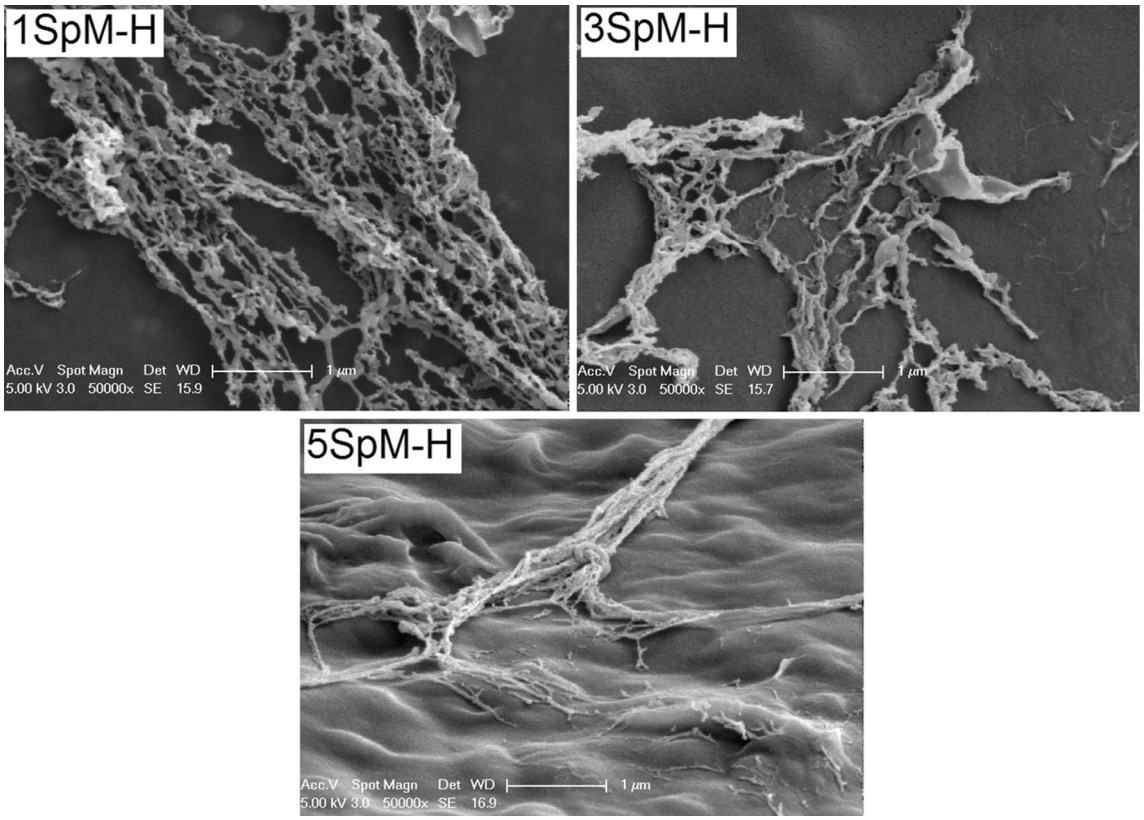

Fig. 7 High magnification (Mag: × 50,000) SEM images of Spirulina networks on the pore walls of the hydrogels

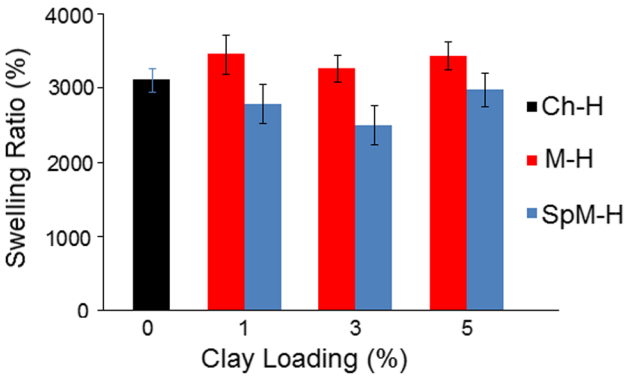

Fig. 8 Percentage swelling of neat chitosan hydrogel (Ch-H), NaMMT loaded composite hydrogels (M-H) and SpMMT loaded composite hydrogels (SpM-H) as a function of clay percentage

value obtained with this composition can be ascribed to the relatively higher number of porous and fewer closed cells obtained by lower degree of the clay loading (Fig. 4). The adsorption of Cr(VI) by NaMMT containing chitosan hydrogels can be based on ion–dipole interactions between the siloxane/silanol groups of the clay and the chromate anions.

On the other hand, chitosan composite hydrogels containing SpMMT clay exhibited higher adsorption performance than NaMMT loaded hydrogels for each clay loading degree (Fig. 9). In particular, 1SpM-H hydrogel was found to have maximum degree of adsorption with an adsorption value of about 48 mg of Cr(VI)/g dry hydrogel in 50 ppm Cr(VI) solution. The adsorption capacity of 1SpM-H hydrogel was found to be about three times those of chitosan and NaMMT loaded chitosan hydrogels. The high adsorption via Sp biosorbent may be ascribed to interaction of chromate ions with hydroxyl, carboxylic, phosphate, amine, amino acids, amide, and sulfate groups of Sp through physical adsorption and ion–dipole interactions. Moreover, in the literature, the pHzpc (pH at zero point charge) value of spirulina was reported to be seven showing that below this pH, surface of the Sp gets positively charged [31]. Therefore, adsorption by Sp can also be due to ionic interactions of chromate anions with protonated amine groups of Sp's protein molecules under the metal adsorption conditions (pH 5.5–6.0) in our study. Moreover, the 1SpM-H as physically crosslinked 3-in-1 type composite hydrogel was found to have 150% higher adsorption capacity, as compared to neat Ch-H hydrogel. In the 3SpM-H and 5SpM-H composite hydrogels, relatively lower adsorption values were obtained, but still higher than neat chitosan hydrogel (Ch-H). This result may be attributed to the functionalized groups of Sp increasing the possible interactions between the MMT layers much more

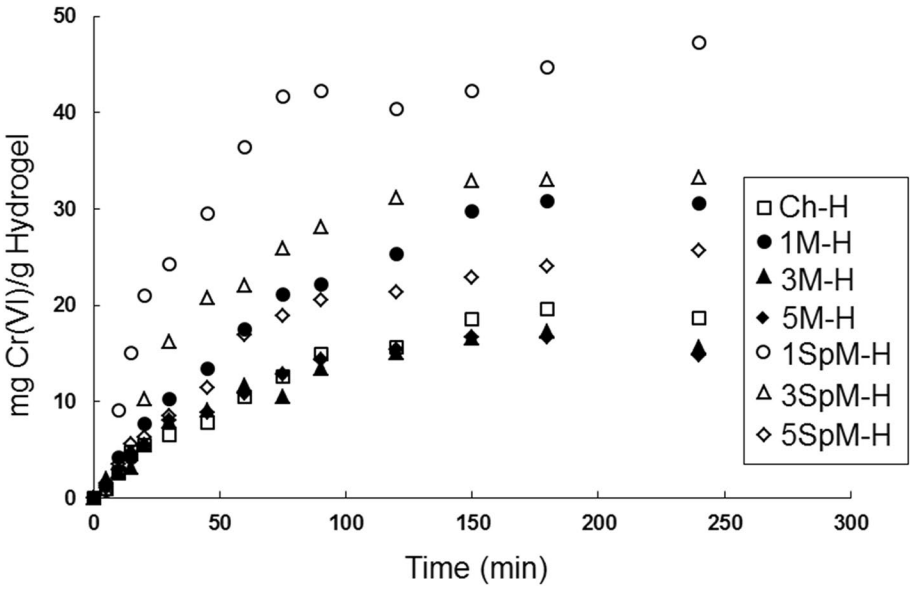

Fig. 9 Metal adsorption capacities of neat hydrogel (Ch-H) and composite hydrogels as a function of time

at their high clay percentages and leading to a more compact clay structure. This was also confirmed with presence of Sp aggregates seen in SEM image of 5SpM-H and partly in that of 3SpM-H (Fig. 6). Moreover, relatively the high adsorption and adsorption rate (first 30 min) obtained by 1 and 3% SpMMT loading can be attributed to Spirulina biosorbent network structure on the surfaces of those composite hydrogels in more open/extended morphology (Fig. 7).

Figures 10 and 11 shows the adsorption kinetics of Cr(VI) on hydrogels and Table 1 indicates the fitting results of pseudo-first order and pseudo-second order models. The experimental adsorption data for neat chitosan hydrogel and NaMMT loaded composite hydrogels, seem to fit pseudo-first-order model much better as compared to pseudo-second-order model. As shown in Table 1, the pseudo-first-order model provided higher correlation coefficient values (R^2) with lower mean relative errors (MRE). Moreover, the adsorption capacities (q_e) determined by pseudo-first-order model were found to be very close to the experimental adsorption capacity ones (q_{exp}) (Table 1) as an indication of reversible physical interactions between Cr(VI)and the hydrogels [32]. On the other hand, the pseudo-second-order model correlates well with the Cr(VI) adsorption data of the SpMMT containing composite hydrogels with higher R^2 and lower MRE values than pseudo-first order one. The adsorption of the Cr(VI) by SpM-H hydrogels can be attributed to abovementioned additional physical and ionic interactions via Sp biosorbent.

Adsorption Isotherms

Adsorption test results were compared by applying Freundlich, Langmuir and Sips isotherm models. Langmuir model is known to be suitable for the equivalent adsorption sites where the molecules are adsorbed in a monolayer of surface having a homogeneous adsorption energy [24, 32]. On the other hand, the Freundlich isotherm is selected for description of the adsorption characteristics for a heterogeneous surface [32, 33]. The Sips isotherm is known to be a combined model involving Freundlich and Langmuir isotherms and obtained via either thermodynamic or equilibrium approximation [14].

In this study, in order to obtain the isotherms and adsorption constants, adsorption experiments were performed in Cr(VI) solutions at four different initial concentrations ranging from 50–200 ppm. The results showed that as the initial metal ion concentration (C_o) increased, each hydrogel adsorbed a larger amount of Cr(VI) (Fig. 12). As it can be seen from Fig. 12 that neat chitosan hydrogel shows an adsorption of 18.69 mg/g for about 75 mg/L Cr(VI) solution whereas the adsorption value was noted to be 35.85 mg/g for the same hydrogel in the solution of 200 mg/L. It is also clear that the hydrogel having the maximum Cr(VI) adsorption for each concentration is 1SpM-H hydrogel. In the literature, the maximum adsorption capacities of MMT and Sp for Cr(VI) were given as 3.61 mg/g [34] and 48.00 mg/g [11] at the concentrations of 500 ppm and 2000 ppm, respectively. In current study, adsorption amount of 1 g of 1SpM-H hydrogel was found to be 78.00 mg at the concentration of 200 ppm (Fig. 12) that is highly remarkable. Moreover, while Sp and MMT by themselves can adsorp only about 4.80% [11] and 0.36% Cr(VI) [34] with respect to their weights, 1SpM-H hydrogel in our case remove 780% Cr(VI) with respect to the weight of SpMMT which makes the current biotechnological process attractive.

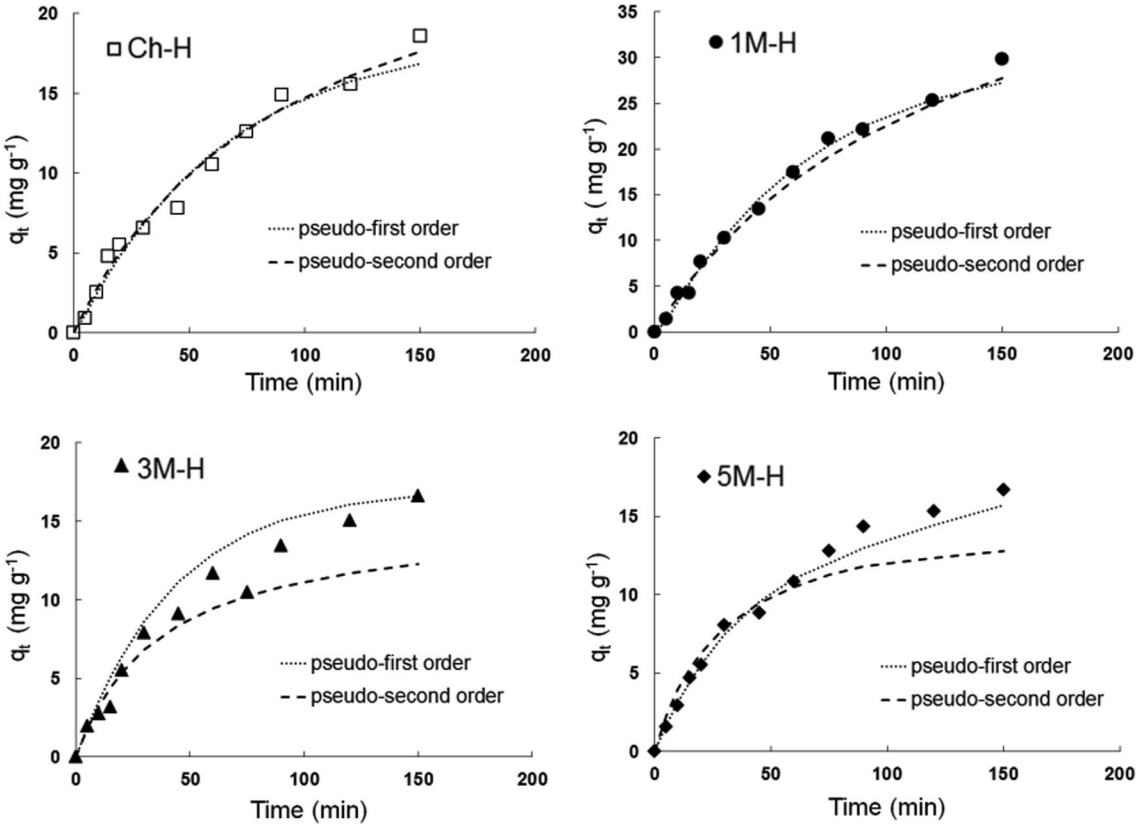

Fig. 10 Kinetic curves for the adsorption of Cr(VI) on neat chitosan and NaMMT loaded composite hydrogels

Figures 13 and 14 gives linear and non-linear adsorption isotherms of metal adsorption capacities of the hydrogels. Table 2 tabulates Freundlich, Langmuir and Sips isotherm parameters for the adsorption. The log q_e–log C_e graph, which gives the Freundlich isotherms is shown in Fig. 13. Freundlich adsorption capacity (K_F) and adsorption intensity (n) values of hydrogels as well as R^2 correlation coefficients were calculated from the isotherms and shown in Table 2. As seen from Table 1, correlation coefficients (R^2) of the hydrogels are very close to one with mean relative error (MRE) values lower than 5%. Therefore, the adsorption behavior of hydrogels was found to be consistent with the Freundlich isotherm. It is clearly seen that the highest adsorption coefficient (K_F) with a value of 4964 belongs to 1SpM-H hydrogel, which is 674% higher than that of neat Ch-H hydrogel. This enhancement is probably resulted from the functional groups of Sp molecules in the hydrogel, being relatively in more open/extended form in the matrix (Fig. 7). This optimized composition in 1SpM-H may provide with active centers to the hydrogel adsorbing the Cr(VI) metal ions more effectively. Since the Cr(VI) ion is generally in the form of $HCrO_4^-$ in aqueous solution in the pH range studied, it can be said that adsorption of the anions by positively charged centers of the matrix polymer and Sp is an effective mechanism for the adsorption. In the Sp containing hydrogels, abovementioned positively charged amine groups of protein molecules of Sp contributes to the adsorption. The chromium ions in the negatively charged form are likely to be more highly adsorbed by the 1SpM-H hydrogel with the presence of abovementioned positively charged groups through physical forces such as electrostatic interactions.

At higher SpMMT loadings (3 and 5%), the excessive amount of Sp was found to decrease Cr(VI) adsorption. The k values of 3SpM-H and 5SpM-H hydrogels were obtained as 2006 and 1215, respectively.The 3SpM-H and 5SpM-H hydrogels have a more porous structure and possible more positively charged amine groups, as compared to 1SpM-H, but exhibit a more compact morphology of Sp networks on their cell walls (Figs. 6 and 7). The less open form of Sp biosorbent which is probably due to insufficient dispersion of the clay layers at higher clay loadings, may reduce the adsorption capacity. The decreased open-net morphology of spirulina can also decrease the maximum amount of its abovementioned receptor sites for the adsorption. It can be assumed that when the amount of SpMMT was increased above 1%, the attractive forces of the SpMMT functional groups, which were in short-distance, increase, leading to

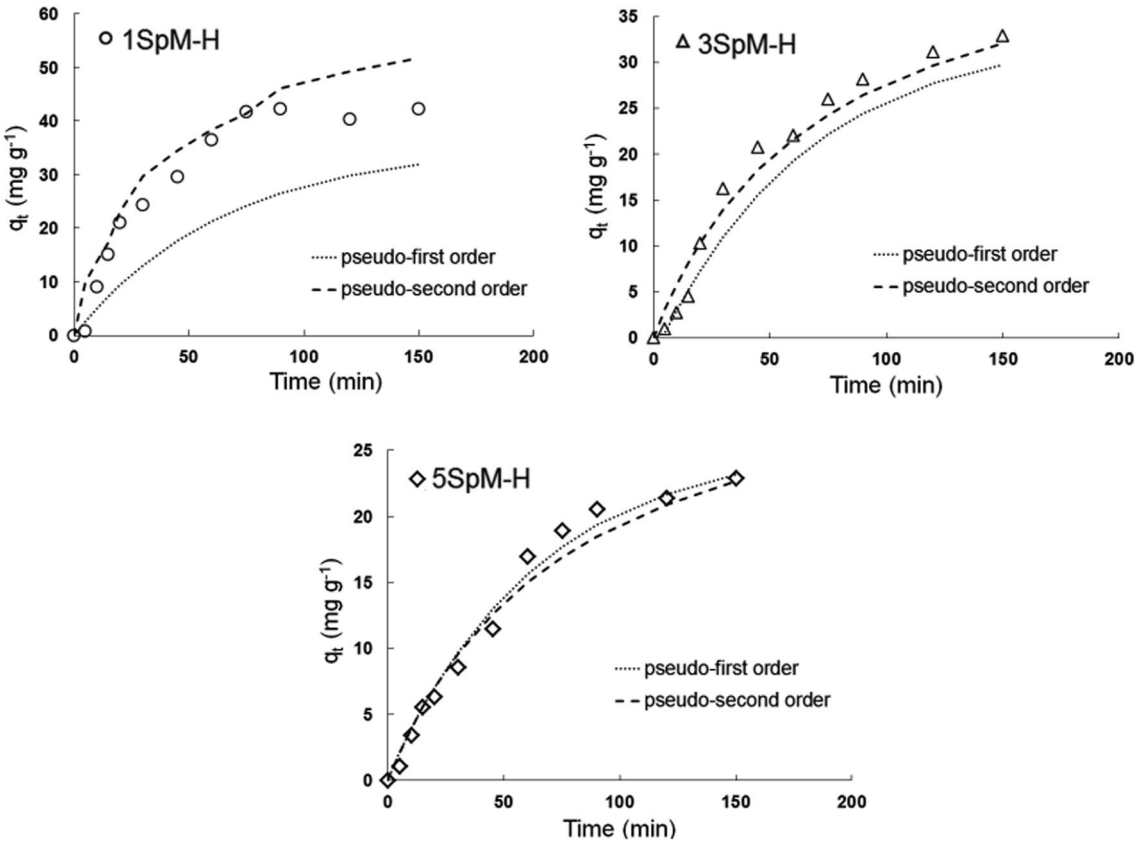

Fig. 11 Kinetic curves for the adsorption of Cr(VI) on SpMMT loaded composite hydrogels

Table 1 Kinetics model parameters for the adsorption on hydrogels

Hydrogels	q_{exp}	Pseudo-first order				Pseudo-second order			
		q_e	k_1	R^2	MRE (%)	q_e	$k_2 \times 10^2$	R^2	MRE (%)
Ch-H	18.67	18.98	0.0157	0.9738	4.02	28.82	0.0365	0.9627	8.01
1 M-H	30.52	31.69	0.0152	0.9947	1.26	50.50	0.0161	0.9377	7.37
3 M-H	15.69	17.09	0.0234	0.9376	7.06	16.67	0.0144	0.9227	19.06
5 M-H	14.23	14.19	0.0249	0.992	2.33	15.74	0.0214	0.9137	15.09
1SpM-H	47.29	35.38	0.0154	0.8751	13.14	68.97	0.0243	0.9637	9.57
3SpM-H	33.30	43.91	0.0271	0.9603	9.23	47.39	0.0296	0.9913	6.37
5SpM-H	25.68	25.39	0.0154	0.9777	5.19	34.48	0.0371	0.9984	4.8

decreased adsorption capacity. At lower SpMMT (1%), on the other hand, Sp forms a looser network structure (Fig. 7), releasing more adsorption sites for the interactions with Cr(VI). For the NaMMT loaded composite hydrogels, the K_F values of NaMMT filled hydrogels except 1 M-H were found to be very low (Table 2). For the 3 M-H and 5 M-H hydrogels, these values were recorded as 0.490 and 0427, respectively. This result can be ascribed to aforementioned possible interaction of positively charged amine groups of the chitosan molecules with negatively charged NaMMT layers, thereby leading to insufficient adsorption of chromate ions and lower K_F values even smaller than neat chitosan hydrogel.

Figure 14 and Table 2 also indicate Langmuir and Sips adsorption isotherms and adsorption parameters, respectively. The results indicate that Langmuir model having a lower range of the correlation coefficient (R^2) values (0.40–0.90) is not suitable for describing the adsorption process. On the other hand, the higher R^2 (0.93–0.99) with low MRE values (lower than 5%) of Freundlich and Sips models indicate that they both fit the experimental data well. Moreover, the maximum adsorption capacity

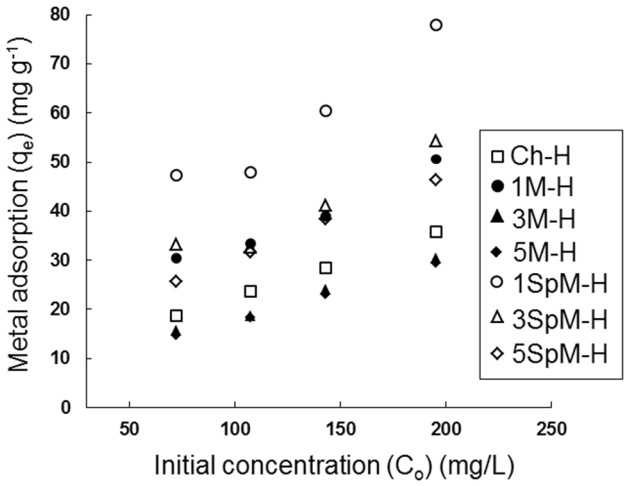

Fig. 12 Influence of initial metal ion concentration on metal adsorption by the hydrogels

according to the Sips model was found to be 3333 mg g^{-1} which belongs to 1SpM-H hydrogel which is in consistent with its experimental kinetic data (Fig. 9) and its Freundlich adsorption capacity value (K_F).

Mechanical Properties of Neat Chitosan and Composite Hydrogels

The moduli of physically cross-linked hydrogels are generally lower than those of chemically crosslinked hydrogels and this low resistance to mechanical deformation limits their application areas [16, 35]. The results of the mechanical compression tests of neat chitosan and composite hydrogels are given in Fig. 15. Figure 15 shows the stress-deformation curves and the data in the low deformation values (0 to 1% deformation range) are shown in Fig. 15-inset figure. All the prepared hydrogels were found to withstand high stress values without breaking. The hydrogels retained their mechanical stability up to 70% deformation. The modulus for the neat chitosan hydrogel without filler was obtained as 0.082 kPa. Compared to neat chitosan hydrogel (Ch-H), an increase in modulus was observed in the composite hydrogels. The modulus was found to increase as the percentage of the clay increases in clay reinforced hydrogels. This can be attributed to the possible ionic and hydrogen bonding interactions of the MMT clay with the polymer matrix leading to restricted chain movements of the polymer matrix [6]. The areas under stress-deformation curves of all the NaMMT reinforced hydrogels, indicating toughness property were found to be lower compared to neat Ch-H hydrogel.

On the other hand, it was found that the modulus value of 1SpM-H (0.416 kPa) composite hydrogel containing 1% SpMMT was about five times higher than that of Ch-H. This result can be attributed to the open web-like Sp morphology obtained with the use of SpMMT at 1% loading (Fig. 7) and increased interaction with matrix, and the relatively closed-pore structure of the composite hydrogel (Fig. 5). When the percentage of SpMMT clay was used above 1%, it was observed that the compression moduli of 3SpM-H (0.227 kPa) and 5SpM-H (0.226 kPa) hydrogels were higher than that of neat chitosan but decreased compared to the 1SpM-H composite hydrogel. The decrease in modulus above 1% SpMMT loading may be attributed to relatively more open porous morphologies of main matrix cells of 3SpM-H and 5SpM-H hydrogels as compared to 1SpM-H (Fig. 5). Also in those composite hydrogels, Sp biomass molecules were found to be in a compact morphology on the cell walls (Figs. 6 and 7), decreasing interactions of the Sp's functional groups with the chitosan matrix. The larger size of open pores and weak Sp-matrix interactions at higher clay loadings can facilitate compressibility with a lower resistance to deformation. More interestingly, 1SpM-H, 3SpM-H and

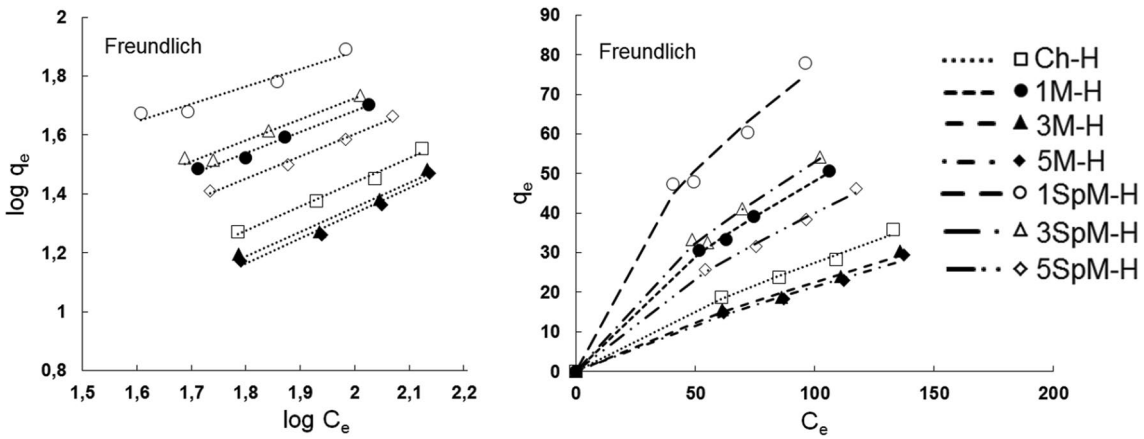

Fig. 13 Linear and non-linear Freundlich isotherms of metal adsorption capacities of the hydrogels

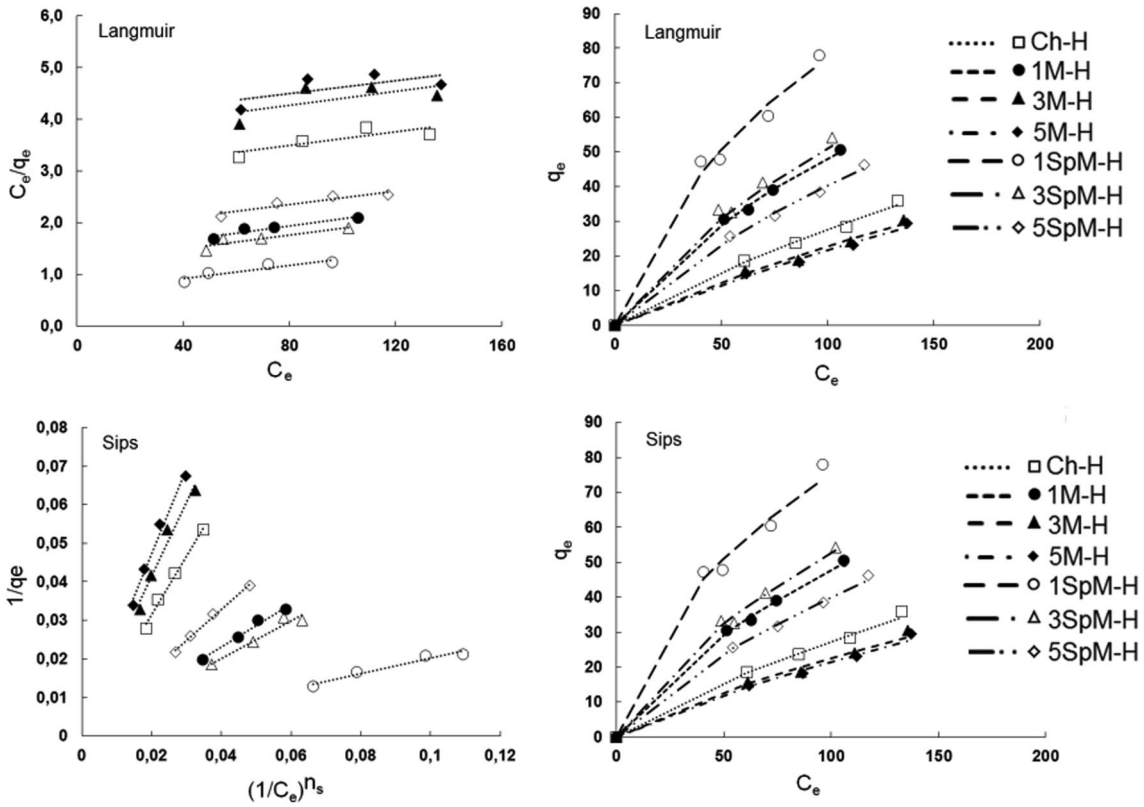

Fig. 14 Linear and non-linear Langmuir and Sips isotherms of metal adsorption capacities of the hydrogels

Table 2 Freundlich, Langmuir and Sips isotherm parameters for the adsorption

Models/Hydrogels	Ch-H	1 M-H	3 M-H	5 M-H	1SpM-H	3SpM-H	5SpM-H
Freundlich model							
K_F (L mg^{-1})	0.641	1.747	0.489	0.426	4.964	2.006	1.215
1/n	0.816	0.720	0.832	0.852	0.594	0.711	0.759
R^2	0.9861	0.9883	0.9659	0.9770	0.9450	0.9651	0.9921
MRE %	2.63	1.74	4.44	3.79	4.76	2.94	1.90
Langmuir model							
K_L (L mg^{-1})$\times 10^3$	2.23	4.875	1.765	1.549	9.39	4.95	3.628
q_m (mg g^{-1})	151.515	147.059	151.515	161.29	158.73	153.846	151.515
R^2	0.6863	0.9032	0.4067	0.4365	0.842	0.8166	0.8703
MRE %	0.69	0.90	0.41	0.44	0.84	0.82	0.87
Sips model							
K_s (L mg^{-1})$\times 10^5$	14.1	5.81	33.7	29.4	9.86	4.51	9.33
ns	0.8158	0.7205	0.8322	0.8517	0.5943	0.7107	0.7594
q_m (mg g^{-1})	909	2000	400	312	3333	2500	1428
R^2	0.9896	0.9838	0.9624	0.9782	0.9323	0.947	0.9924
MRE %	2.62	1.85	4.40	3.21	4.53	3.03	1.90

5SpM-H hydrogels showed higher toughness values of 3.74, 3.72 and 2.43 N mm, respectively, in comparison with that of neat Ch-H hydrogel (2.35 N mm). This can be due to increased viscous character due to reversible and physical polymer–clay interactions in presence of SpMMT clay [26, 36].

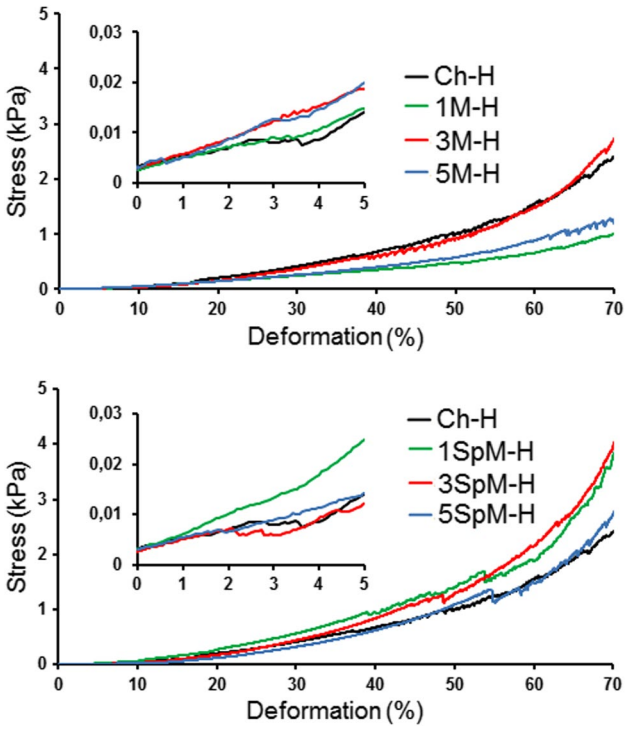

Fig. 15 Compression stress-deformation curves for neat Ch-H and the composite hydrogels. Inset figure indicates the deformation percentage range of 0–5%, showing changes in compression modulus

Conclusions

Immobilization of Spirulina biosorbent/biomass onto surface of montmorillonite (MMT) layered silicate was done via help of lyophilization based "cryoscopic expansion" (C-XP) method, and organophilic SpMMT clay was obtained. SpMMT loaded hydrogels showed higher adsorption capacities than those including NaMMT clay at each loading degrees. The physically crosslinked "3-in-1 type" composite hydrogel containing 1% SpMMT was found to have 150% more adsorption capacity, as compared to neat chitosan hydrogel. It is thought that the open fish-net morphology of Sp on MMT clay on the walls of SpMMT clay containing composite hydrogels provides its more functional groups as receptors for Cr(VI) metal ions. The adsorption kinetic data of the NaMMT loaded hydrogels was correlated with pseudo-first order model and that of SpMMT clay containing hydrogels agreed well with the pseudo-second order model. For all the hydrogels, the adsorption isotherms exhibited a good fit for the Freundlich model and Sips model with maximum adsorption capacity of 3333 mg g^{-1} for 1% SpMMT containing composite hydrogel. The mechanism of high adsorption capacity via the composite hydrogels involving Spirulina biosorbent could be realized by the interactions of chromate ions with special Sp network structure in open form presenting more adsorption sites for the Cr(VI). For the composite hydrogels containing Sp, the compression modulus together with toughness were found to increase in comparison with neat chitosan hydrogel and NaMMT containing composite hydrogels. This is attributed to high interactions of Sp and MMT functional groups with chitosan polymer through abovementioned additional functional groups of Sp biosorbent/biomass.

Acknowledgements The financial support provided by Yalova University Scientific Research Projects Coordination Department (project no. 2015/BAP/117) is gratefully acknowledged.

Compliance with Ethical Standards

Conflict of interest The authors declare that they have no conflict of interest.

References

1. Yusof AM, Malek NANN (2009) J Hazard Mater 162:1019
2. Bai S, Abraham TE (2001) Bioresour Technol 79:73
3. Prigione V, Zerlottin M, Refosco D, Tigini V, Anastasi A, Varese GC (2009) Bioresour Technol 100:2770
4. Gupta V, Rastogi A (2009) J Hazard Mater 163:396
5. Maryuk O, Pikus S, Majdan M, Skrzypek H, Zięba E (2005) Mater Lett 59:2015
6. Aydınoğlu D, Akgül Ö, Bayram V, Şen S (2014) Polym Plast Technol Eng 53:1706
7. Nasernejad B, Zadeh TE, Pour BB, Bygi ME, Zamani A (2005) Process Biochem 40:1319
8. Tekay E, Şen S, Aydınoğlu D, Nugay N (2016) e-Polymers 16:15–24
9. Arunakumara K, Zhang X, Song X (2008) JOUC 7:397
10. Chojnacka K, Chojnacki A, Gorecka H (2005) Chemosphere 59:75
11. Doshi H, Ray A, Kothari I (2007) Biotechnol Bioeng 96:1051
12. Wang W, Zhao Y, Yi H, Chen T, Kang S, Li H, Song S (2017) Nanotechnology 29:025605
13. Kang S, Zhao Y, Wang W, Zhang T, Chen T, Yi H, Rao F, Song S (2018) Appl Surf Sci 448:203
14. Wang W, Zhao Y, Bai H, Zhang T, Ibarra-Galvan V, Song S (2018) Carbohydr Polym 198:518
15. Hoffman AS (2012) Adv Drug Deliv Rev 64:18
16. Wang X, Du Y, Luo J, Lin B, Kennedy JF (2007) Carbohydr Polym 69:41
17. Wang M (2003) Biomaterials 24:2133
18. Kithva P, Grøndahl L, Martin D, Trau M (2010) J Mater Chem 20:381
19. Lavorgna M, Piscitelli F, Mangiacapra P, Buonocore GG (2010) Carbohydr Polym 82:291
20. Tang C, Xiang L, Su J, Wang K, Yang C, Zhang Q, Fu Q (2008) J Phys Chem B 112:3876
21. Díaz-Visurraga J, Melendrez M, Garcia A, Paulraj M, Cardenas G (2010) J Appl Polym Sci 116:3503
22. Yang X, Tu Y, Li L, Shang S, Tao X (2010) ACS Appl Mater Interfaces 2:1707
23. Mert HH, Tekay E, Nugay N, Nugay T, Şen S (2018) Polym Eng Sci 58:1229
24. Kummer G, Schonhart C, Fernandes M, Dotto G, Missio A, Bertuol D, Tanabe E (2018) J Polym Environ 26:4073

25. Eaton ADCLS, Greenberg AE, Franson MAH (2005) In: Eaton AD (ed) Standard methods for the examination of water and wastewater. American public health association, Washington DC, p 49
26. Palantöken S, Tekay E, Şen S, Nugay T, Nugay N (2016) Polym Compos 37:2770
27. Tu J, Cao Z, Jing Y, Fan C, Zhang C, Liao L, Liu L (2013) Compos Sci Technol 85:126
28. Liu M, Wu C, Jiao Y, Xiong S, Zhou C (2013) J Mater Chem B 1:2078
29. Ansari R, Delavar AF (2010) J Polym Environ 18:202
30. Vachoud L, Zydowicz N, Domard A (1997) Carbohydr Res 302:169
31. Dotto G, Lima E, Pinto L (2012) Bioresour Technol 103:123
32. Mahl CR, Taketa TB, Bataglioli RA, de Arruda EJ, Beppu MM (2018) J Polym Environ 26:4338
33. Theivarasu C, Mylsamy S (2010) Int J Eng Sci Technol 2:6284
34. Akar ST, Yetimoglu Y, Gedikbey T (2009) Desalination 244:97
35. Hoffman AS (2002) Adv Drug Deliv Rev 54:3
36. Helvacıoğlu E, Aydın V, Nugay T, Nugay N, Uluocak BG, Şen S (2011) J Polym Res 18:2341